J Ind Microbiol Biotechnol (2004) 31: 311–322
DOI 10.1007/s10295-004-0151-8

ORIGINAL PAPER

Gareth Lewis · Ian W. Taylor · Alvin W. Nienow
Christopher J. Hewitt

The application of multi-parameter flow cytometry to the study of recombinant *Escherichia coli* batch fermentation processes

Received: 11 February 2004 / Accepted: 26 May 2004 / Published online: 13 July 2004

Abstract Multi-parameter flow cytometric techniques coupled with dual colour fluorescent staining were used to study the physical and metabolic consequences of inclusion body formation in batch cultures of the recombinant *Escherichia coli* strain MSD3735. This strain contains a plasmid coding for the isopropylthiogalactopyranoside-inducible model eukaryotic protein AP50. It is known that the synthesis of foreign proteins at high concentrations can exert a severe metabolic stress on the host cell and that morphological changes can occur. In this work, using various points of induction, it was shown that inclusion body formation is followed immediately by measurable changes in the characteristic intrinsic light scatter patterns for the individual cell (forward scatter, 90° side scatter) and a concomitant progressive change in the individual cell physiological state with respect to both cytoplasmic membrane polarisation and permeability. This work establishes flow cytometry as a potentially valuable tool for monitoring recombinant fermentation processes, providing important information for scale-up. Further, we discuss the possibility of optimising inclusion body formation by manipulating the fermentation conditions based on these rapid ''real-time'' measurements.

Keywords Flow cytometry · *Escherichia coli* · Fermentation · Membrane integrity · Membrane potential · Inclusion bodies

G. Lewis · A. W. Nienow · C. J. Hewitt (✉)
School of Engineering (Chemical Engineering),
The University of Birmingham, Edgbaston,
B15 2TT, UK
E-mail: c.j.hewitt@bham.ac.uk.
Tel.: +44-121-4145287
Fax: +44-121-4145324

I. W. Taylor
AstraZeneca, Mereside,
Alderly Park, Macclesfield, Cheshire,
SK10 4TG, UK

Introduction

The ability to cultivate bacterial strains, expressing heterologous recombinant proteins, to high cell density is an increasingly important technique throughout the field of biotechnology, from basic research programmes (structural or kinetic studies) to large-scale pharmaceutical production processes [4]. *Escherichia coli* remains one of the most attractive organisms for the production of recombinant proteins where no complex post-translational modifications (e.g. glycosylation or disulfide bond formation) are required for biological activity, because its genetics and physiology are well understood. Indeed, continued developments in this area have resulted in expression systems that produce foreign proteins in quantities of up to 50% of the total cell protein [1]. The process of scaling-up such a system is often the last step in a research and development programme leading to the industrial scale synthesis of recombinant products by fermentation [6].

In a recent series of papers, we discussed the effect on process performance of the different physiological stresses imposed on an *E. coli* cell during a whole range of fermentation processes and importantly at various scales of cultivation (5–20,000 l). First, we compared batch, fed-batch and continuous culture fermentations [10, 11]. This work demonstrated that, whilst fed-batch fermentations, as expected, produced a much higher biomass, multi-parameter flow cytometry indicated a relatively high proportion (ca. 16%) of dead cells present at the end of the fermentation. In contrast, during batch and continuous culture fermentations, cell viability was found to be almost 100% throughout. This result was discussed in terms of the severe stress imposed upon cells by an ever-increasing level of glucose limitation during the relatively long (37 h) fed-batch process. However, these initial studies were carried out in a well mixed laboratory-scale 5-l vessel, where it can be assumed that spatial heterogeneities with respect to dissolved oxygen, glucose and pH (even in the fed-batch case) do not exist

[18]. With increasing scale, at equal levels of agitation intensity (expressed as x W/kg, with typical large-scale values being of the order of 2–3 W/kg), the assumption of homogeneity with respect to dissolved oxygen (dO_2) concentration in batch or fed-batch fermentations [20], or for dO_2 and glucose in the fed-batch case [5], can no longer be justified. Further, it has now been shown that chemical concentration gradients exist in large-scale bioreactors [23] and that cells circulating around a large-scale bioreactor respond rapidly to such a changing micro-environment by the fast transcriptional induction of an alternative set of genes [21]. Therefore, in our next papers [7, 12, 19], the problems associated with scale-up were investigated. It was shown that a changing micro-environment with respect to pH, glucose and dO_2 during high cell density fed-batch fermentations had a profound effect on cell physiology and hence on viable biomass yield. These studies were carried out at both production (20,000 l) and laboratory (5 l) scale. These results were then compared with those from a series of scaled-down predictive experimental models (5 l) of the production scale, where the difficulty of achieving good mixing (broth homogeneity) as found at the production scale was simulated by a two-compartment model. This work revealed that a progressive change in the cell physiological state (with respect to cytoplasmic membrane polarity and integrity) generally occurs throughout the course of a fed-batch fermentation and that the extent of these changes was dependent on the scale of cultivation. Further, it showed that the relatively poorly mixed conditions in the large-scale bioreactor led to a low biomass yield but a high cell viability (with respect to cytoplasmic membrane permeability) and, conversely, the small-scale well mixed fermentation gave the highest biomass yield but the lowest cell viability.

However, all of these studies were carried out using the untransformed wild-type bacterial strain, *E. coli* W3110. So, this work does not take into account the additional physiological stress imposed on a cell by having to synthesise a foreign protein when trying to predict process performance on scale-up. It is known that the synthesis of foreign proteins at high concentrations exerts a severe metabolic stress on the host cell [2, 3]. The consumption of essential substrates (e.g. amino acids) and energy is switched away from normal cellular functions, resulting in a reduction or cessation of growth and in extreme cases cell death. Therefore, in this work, we compare the performance of the untransformed host *E. coli* BL21 (DE3; culture collection accession number MSD2052) with the recombinant *E. coli* BL21 (DE3; culture collection accession number MSD3735) in batch culture, using multi-parameter flow cytometry. *E. coli* MSD3735 contains a plasmid coding for an isopropylthiogalactopyranoside (IPTG)-inducible model mammalian protein AP50 encoding amino acids 164–435 with a N-terminal His_6-cmyc fusion tag, under the control of a T7 RNA promoter and a tetracycline resistance marker [8]. The recombinant system used here is further complicated because, under normal growth conditions, the protein can be mis-folded, accumulating in the form of insoluble, phase-bright, biologically inactive, so-called ''inclusion bodies'' in the cytoplasm of the cell. In this way, the effect of any physiological or physical stress imposed by the synthesis of AP50 in addition to that imposed by a batch fermentation process could be investigated and used as the basis for future studies investigating the scale-up of a model industrial process.

Methods and materials

The recombinant strain of *E. coli* MSD3735 and the untransformed host *E. coli* MSD2052 were obtained from AstraZeneca (Alderly Park, Macclesfield, UK). Both organisms were maintained at −80°C in Luria Bertani (LB), broth (Difco, Nottingham, UK) supplemented with equal volumes of 2× cryogen solution containing (per litre): 3.6 g KH_2PO_4, 12.6 g K_2HPO_4, 0.9 g tri-sodium citrate, 1.8 g $(NH_4)_2SO_4$ and 300 g glycerol. A filter-sterilised aqueous solution (10 ml) of $MgSO_4{\cdot}7H_2O$ (0.18 g/l) was added aseptically after autoclaving the medium. The composition of the high yeast extract growth medium used for batch fermentations was (per litre of distilled water): 3.0 g KH_2PO_4, 6.0 g Na_2HPO_4, 05 g NaCl, 2.0 g casein hydrolysate, 10.0 g $(NH_4)_2SO_4$, 35 g glycerol and 20 g yeast extract. After the medium had cooled, the following post-sterilisation additions were made (final concentration per litre): 0.5 g $MgSO_4$, 0.0294 g $CaCl_2{\cdot}H_2O$, 0.008 g thiamine, 0.040 g/0.020 g $FeSO_4$/citric acid and 0.5 ml/l of a trace elements stock solution. The trace elements stock solution was made up in distilled water as follows (per litre): 0.2 g $AlCl_3{\cdot}6H_2O$, 0.08 g $CoCl_2{\cdot}6H_2O$, 0.02 g $CrK(SO_4){\cdot}12H_2O$, 0.02 g $CaCl_2$, 0.01 g H_3BO_3, 0.2 g KI, 0.26 g $MnSO_4{\cdot}4H_2O$, 0.009 g $NiSO_4{\cdot}7H_2O$ and 0.04 g $NaMoO_4$. Tetracycline (10 mg/l) was added to the growth medium for fermentations with the recombinant organism MSD3735. IPTG (0.5 mM) was added aseptically according to the experimental protocol to induce expression of AP50. Chemicals used were of reagent grade.

Batch fermentations were carried out in a 5-l cylindrical glass bioreactor (162 mm diam., 300 mm total height), with a working volume of 4 l. The vessel was fitted with two 82-mm, six-bladed paddle-type impellers situated 80 mm apart with the bottom impeller 80 mm above the bottom of the vessel. The vessel was fitted with four equally spaced baffles, width 15 mm and equipped with controls for dO_2, pH, anti-foam, temperature and impeller speed. The temperature was maintained at 37°C, the airflow rate was 1 vvm and the impeller speed was varied in order to maintain dO_2 above the 50% saturation level. pH was controlled above 6.7 using 2 M NaOH. Polypropylene glycol 2,025 was used, on demand, to control foaming. dO_2 was measured continuously using a polargraphic steam-sterilisable oxygen electrode (Ingold). A 2% inoculum was prepared by growing the culture on LB medium (50 ml) in a 500-ml Erlenmeyer shake-flask for 13 h at 37°C and 300 rpm.

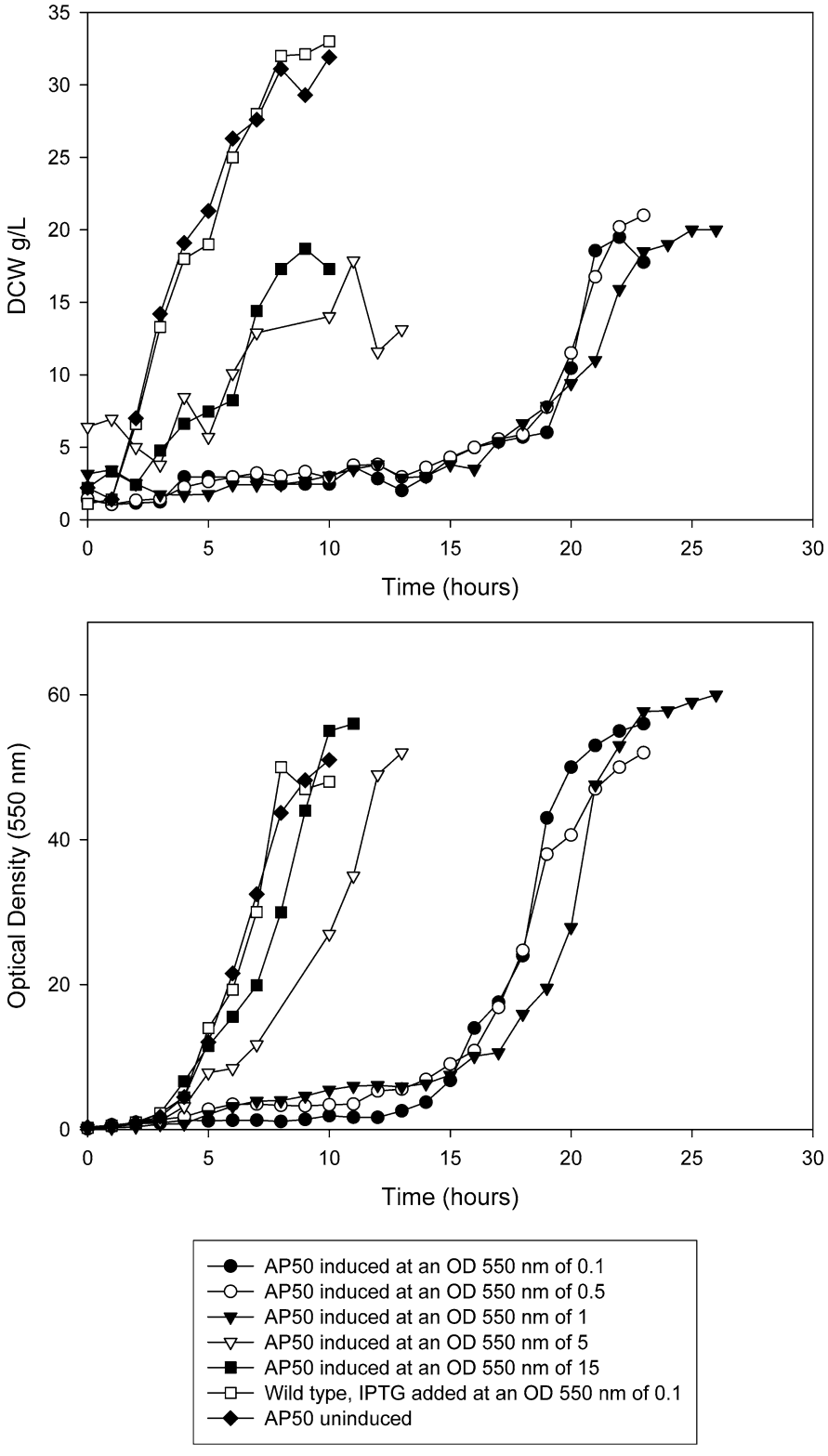

Fig. 1 OD_{550} and DCW profiles for a series of batch fermentations where the point of induction of AP50 synthesis was varied by the addition of 0.5 mM IPTG at different OD_{550}

Flow cytometry

The advantages of multi-parameter flow cytometry over more conventional microbiological techniques such as dilution plating (colony-forming units/ml) are well documented [13, 17], but briefly, using various mixtures of fluorescent dyes, it is possible to resolve the physiological state of an individual microbial cell beyond culturability, based on the presence or absence of an intact polarised cytoplasmic membrane and the transport mechanisms across it, enabling assessment of population heterogeneity. For all fermentations, flow

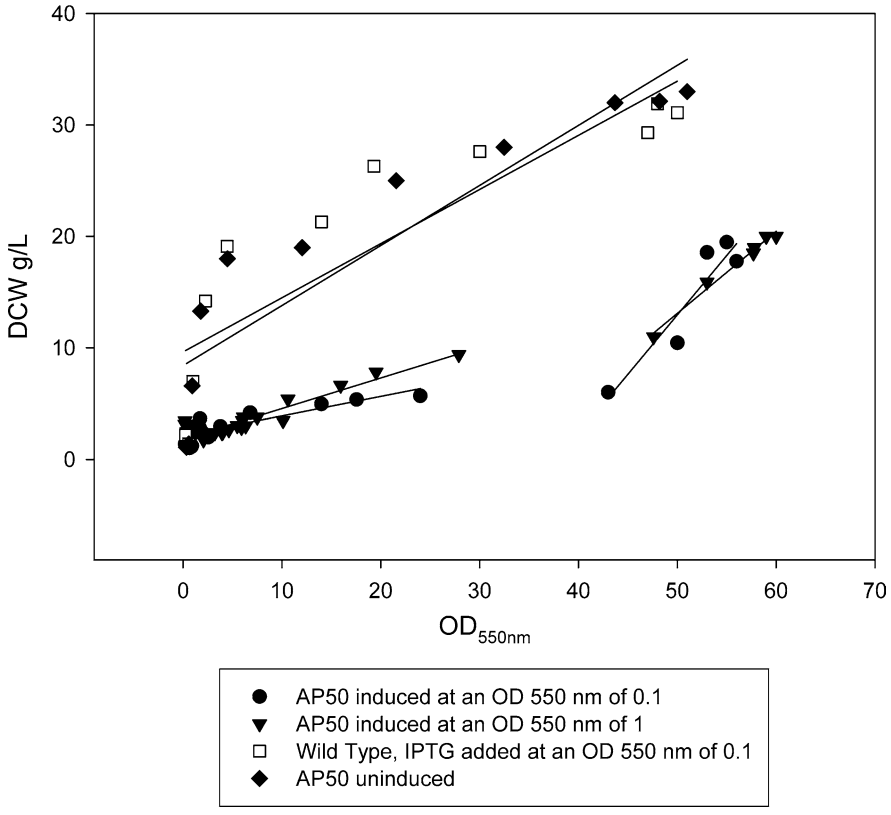

Fig. 2 Correlation (by linear regression) between OD_{550} and DCW for: (1) AP50 uninduced ($y = 8.41 + 0.54x$, $R = 83.5\%$), (2) wild type where 0.5 mM IPTG was added at $OD_{550} = 0.1$ ($y = 2 + 0.68x$, $R = 81.0\%$), (3) AP50 induced at $OD_{550} = 0.1$ for $OD_{550} < 40$ ($y = 2.15 + 0.174x$, $R = 72\%$), (4) AP50 induced at $OD_{550} = 0.1$ for $OD_{550} > 40$ ($y = -40 + 1.07x$, $R = 88\%$), (5) AP50 induced at $OD_{550} = 1.0$ for $OD_{550} < 40$ ($y = 1.82 + 0.274x$, $R = 89\%$) and (6) AP50 induced at $OD_{550} = 1.0$ for $OD_{550} > 40$ ($y = -23.62 + 0.73x$, $R = 98\%$)

cytometric measurements were made using a Coulter Epics Elite analyser with 488 nm excitation from an argon-ion LASER at 15 mW. Samples taken from the culture were immediately diluted with Beckman Coulter Isoton II and stained with a mixture of two fluorescent dyes, propidium iodide (PI) and bis-(1,3-dibutylbarbituric acid) trimethine oxonol (BOX), i.e. PIX staining. Stock solutions of each dye were prepared as follows: PI was made up at 200 μg/ml in distilled water and BOX was made up at 10 mg/ml in dimethylsulphoxide (DMSO). The DMSO stock solution was maintained at −20°C and the distilled water stock solution was maintained at 4°C. The working concentrations of PI and BOX were 5 μg/ml and 10 μg/ml respectively in Dulbecco's buffered saline (DBS, pH 7.2). In order to facilitate staining with BOX, 4 mM EDTA was added to the working solution. The working solution (10 μl) was then added to approximately 1 ml of the appropriately diluted cell sample suspension for staining. All solutions were passed through a 0.2-μm filter immediately prior to use, to remove particulate contamination. Optical filters were set up as standard for the Coulter Epics Elite analyser [16] to measure PI fluorescence at 630 nm and BOX fluorescence at 525 nm. Since there is a spectral overlap between BOX- and PI-emitted fluorescence, the software compensation was set up in such a way that BOX-emitted fluorescence was eliminated from the PI-emitted fluorescence detector and vice versa.

Transmission electron microscopy

A cell sample (1 ml) was centrifuged at 9,000 *g* in a laboratory-scale centrifuge (MSE, UK) for 10 min and resuspended in 2.5% glutaraldehyde in 0.1 M phosphate buffer (pH 7.2) for 1 h. The sample was again centrifuged (9,000 *g*) for 10 min and resuspended in 1% osmium tetroxide in 0.1 M phosphate buffer (pH 7.2) for 1 h. The fixed cells were dehydrated sequentially in graded aliquots (70, 90, 100, 100, dried 100%) of ethanol and embedded in a 1:1 mixture of propylene oxide/Araldite resin. The resin was de-gassed and allowed to polymerise at 60°C for 16 h. Ultra-thin sections (70 nm) were cut using a Reichart–Jung Ultracut E microtome and stained with uranyl acetate and Reynolds lead citrate. The samples were then examined using a Jeol Ex transmission electron microscope (TEM) with an accelerating voltage of 80 kV.

Additional analytical techniques

The cell biomass was measured by optical density at 550 nm (OD_{550}) in a double-beam spectrophotometer, calibrated against dry cell weight (DCW) at 100°C to constant weight. For plasmid stability tests, samples were taken and serially diluted with DBS; and 0.1 ml of the resulting suspension was plated onto nutrient agar supplemented with 10 mg/l tetracycline and incubated at 37°C for 24 h.

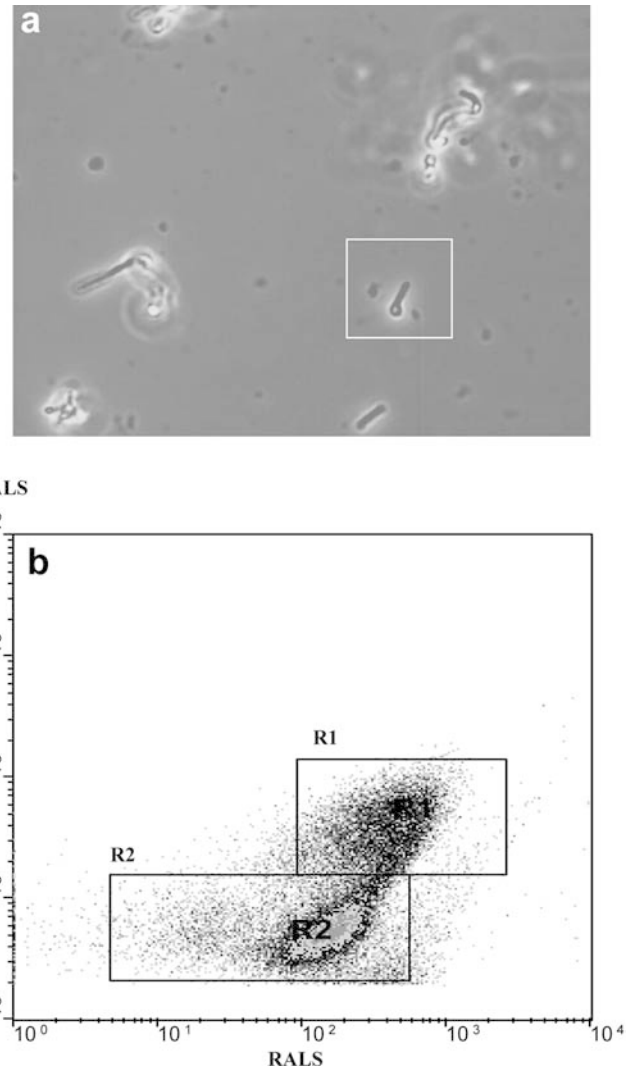

Fig. 3a Light micrograph (×40) of a recombinant *E. coli* MSD3735 cell expressing AP50 as an insoluble inclusion body. **b** Intrinsic light scattering (FALS vs RALS) for an *E. coli* MSD3735 population, a proportion of which is producing AP50 as an inclusion body (*R1*) and a proportion of which is not (*R2*)

The glycerol concentration was measured using a Gilson HPLC system with an aminex HPX-87P analysis column (Bio-Rad, UK), using 0.5 mM H_2SO_4 as the mobile phase, with a flow rate of 6 ml/min, resulting in a retention time of 13.4 min.

For recombinant protein AP50 analysis, suitable broth samples were centrifuged for 10 min, the supernatant discarded and each pellet re-suspended in double-strength lysis buffer made up as follows: 375 g (30%) sucrose, 37.5 g 1 M Tris-HCl and 187.5 g 0.4 M EDTA in deionised water to 750 ml (pH 8), ensuring an equal biomass concentration in each sample. To the resultant suspension, 1.25 mg/ml hen egg lysozyme was added and held on ice for 30 min. This was then sonicated at 50% amplitude on ice for consecutive pulses of 30 s, until microscopic examination showed >95% of the cells had been disrupted. Of this, 150 µl were taken for total cell protein analysis. A further 1 ml was centrifuged at 13,000 rpm to separate the insoluble and soluble fractions. The resulting supernatant (150 µl) and the re-suspended pellet were used for soluble and insoluble protein analysis, respectively. SDS-PAGE analysis [14] was used to determine the percentage total soluble and insoluble cell protein, using a 12.5% separation gel. Each of the samples received 150 µl of Laemmli loading buffer and 10 µl were loaded per lane. Protein was stained with Coomassie brilliant blue R-250; and low molecular weight protein markers (Amersham Pharmacia Biotech, Buckinghamshire, UK) were used to identify AP50 (35 kDa).

Results and discussion

Two series of batch fermentations were carried out: (1) with the untransformed host *E. coli* MSD2052 strain and (2) with the recombinant *E. coli* MSD3735 strain. The timing of the addition of the inducing agent (IPTG) was varied dependent on the OD_{550} of the culture, within the range $OD_{550} = 0.1–15.0$. In addition, control experiments were carried out where IPTG was added to a batch fermentation of the untransformed host at $OD_{550} = 0.1$ and was not added at all to a batch fermentation of the recombinant strain. Reproducible measurements of pH, dO_2, OD_{550}, DCW and [glycerol] were made (Fig. 1, not all data shown). Additionally, during the course of each fermentation, individual cell physiology was measured by multi-parameter flow cytometry. Batch fermentations were terminated when the glycerol was exhausted and a DCW of 17–34 g/l was achieved. The point of induction had a clear effect on fermentation progression, as measured by OD_{550} and DCW profiles (Fig. 1). In all cases, the profiles of glycerol utilisation and dO_2 were the opposite of the OD_{550} and DCW profiles. Whilst the maximum specific growth rates for all fermentations (estimates made using DCW measurements only) were comparable (0.46–0.51 per hour), the time of termination and final DCW differed. For fermentations where induction occurred in the range $OD_{550} = 0.1–1.0$, glycerol was exhausted at between 20 h and 25 h whereas, for all recombinant fermentations either not induced or induced at $OD_{550} = 15$ or where IPTG was added to a batch fermentation of the untransformed host at $OD_{550} = 0.1$, the glycerol was exhausted after ca. 12 h. Interestingly, the relationship between OD_{550} and DCW seems to be very complex (Fig. 2). Whilst, in all cases, the final OD_{550} for each fermentation was similar (ca. 58–60) the final DCW for those fermentations where the recombinant protein is expressed was approximately half (ca. 17 g/l) that (ca. 34 g/l) of those fermentations where the protein was not expressed. This drop in final DCW is not entirely unexpected, since energy is presumably being redirected away from cell growth towards protein synthesis in producing cultures. Importantly however, the synthesis or accumulation of the recombinant protein must also

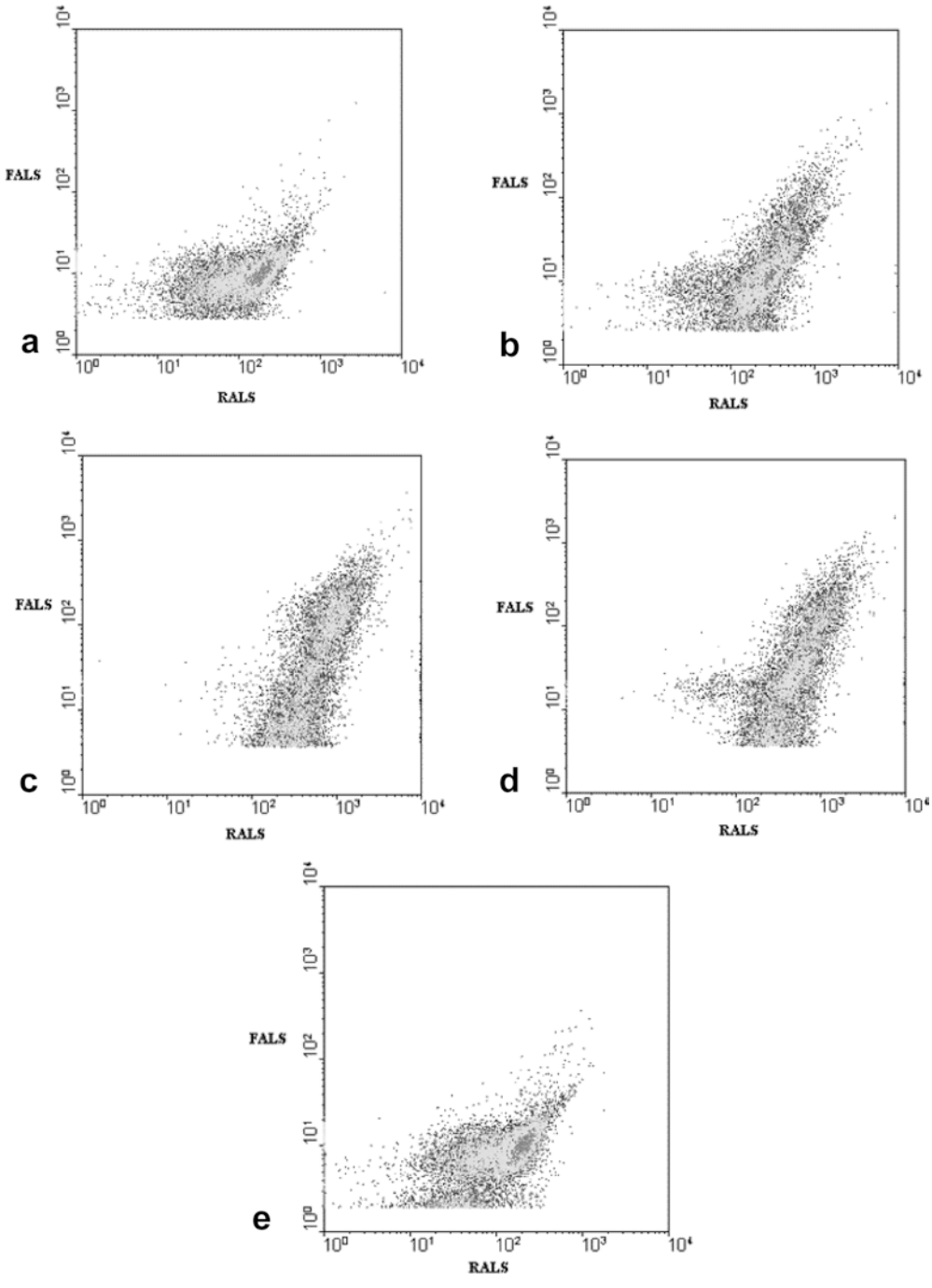

Fig. 4 a–e Changes in the intrinsic light scattering for *E. coli* MSD3735 during the course of a batch fermentation where synthesis of AP50 was induced at $OD_{550} = 1$. **a** Immediately before induction, **b** ca. 1 h after induction, **c** 3 h, **d** 15 h, **e** 20 h. This illustrates the change from the bimodal clustering characteristic for rod-shaped cells towards a more diffuse cluster representing cells producing inclusion bodies and the change back again

affect broth turbidity, i.e. cell suspensions producing recombinant protein must transmit less light, for the final OD_{550} measurements to remain the same for all fermentation processes. Additionally, for those cultures producing recombinant protein, the DCW/OD_{550} relationship changes for $OD_{550} > 40$. This seems to be independent of inclusion body formation, since a similar DCW/OD_{550} correlation is found for all fermentations expressing recombinant protein, whether inclusion bodies are formed or not. (Fig. 2, not all data shown). The reasons are not known but this highlights the danger of relying solely on OD measurements when following the biomass concentration during fermentation processes. Why the OD at which IPTG is added has such an effect is uncertain; but, since the IPTG concentration is kept the same (0.5 mM) for each fermentation, we know that the concentration of IPTG per individual cell at the exact time of IPTG addition is very different. Therefore, at low OD, the induction effect may be stronger than at higher OD. This may lead to a greater level of expression of the protein and a greater stress for the individual cell. Unfortunately, there is no reliable assay for AP50 quantification, so expression level data are not available. Since the addition of IPTG to the non-

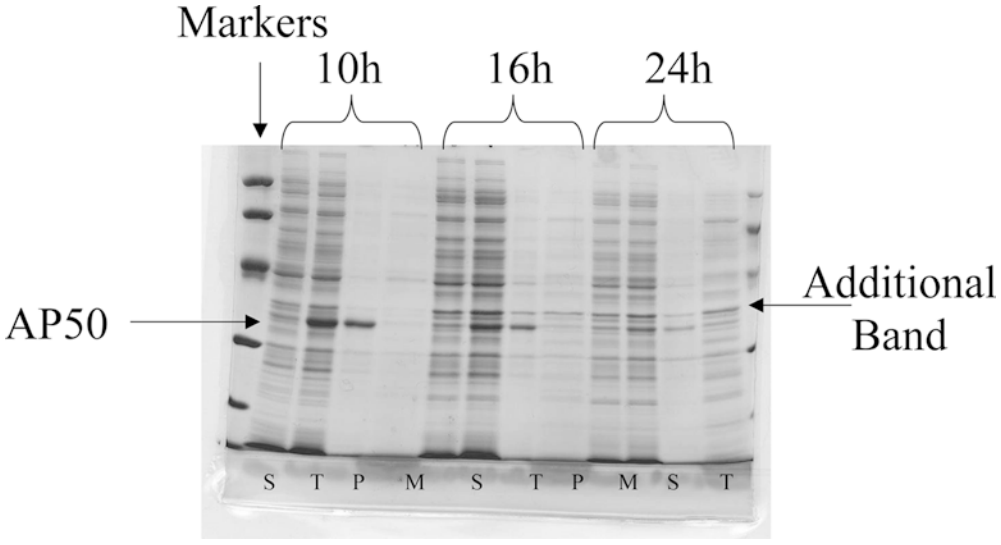

Fig. 5 SDS-PAGE gel analysis of cell samples taken at 10, 16 and 24 h during the course of a batch fermentation where synthesis of AP50 was induced at $OD_{550} = 1$. This was used to determine the ratio of soluble to insoluble AP50. Low molecular weight protein markers (Amersham Pharmacia Biotech) were used to identify AP50 (35 kDa). An additional unidentified protein band can also clearly be seen, the appearance of which coincides with the disappearance of the band associated with AP50

recombinant fermentation had no effect on fermentation progression, any toxic effects can be largely discounted.

Light scatter

In principle, it should be possible to detect inclusion body formation based on changes in the intrinsic light scatter measurements alone [9, 22]; and in some cases a linear relationship has been shown to exist between forward angle light scatter (FALS) and insoluble protein accumulation [15]. When the cell passes through the laser beam, scattered light is detected in two planes. FALS is detected in the plane of the beam and is often quoted as being a measure of relative cell size. Right angle light scatter (RALS) is collected at 90° to the beam

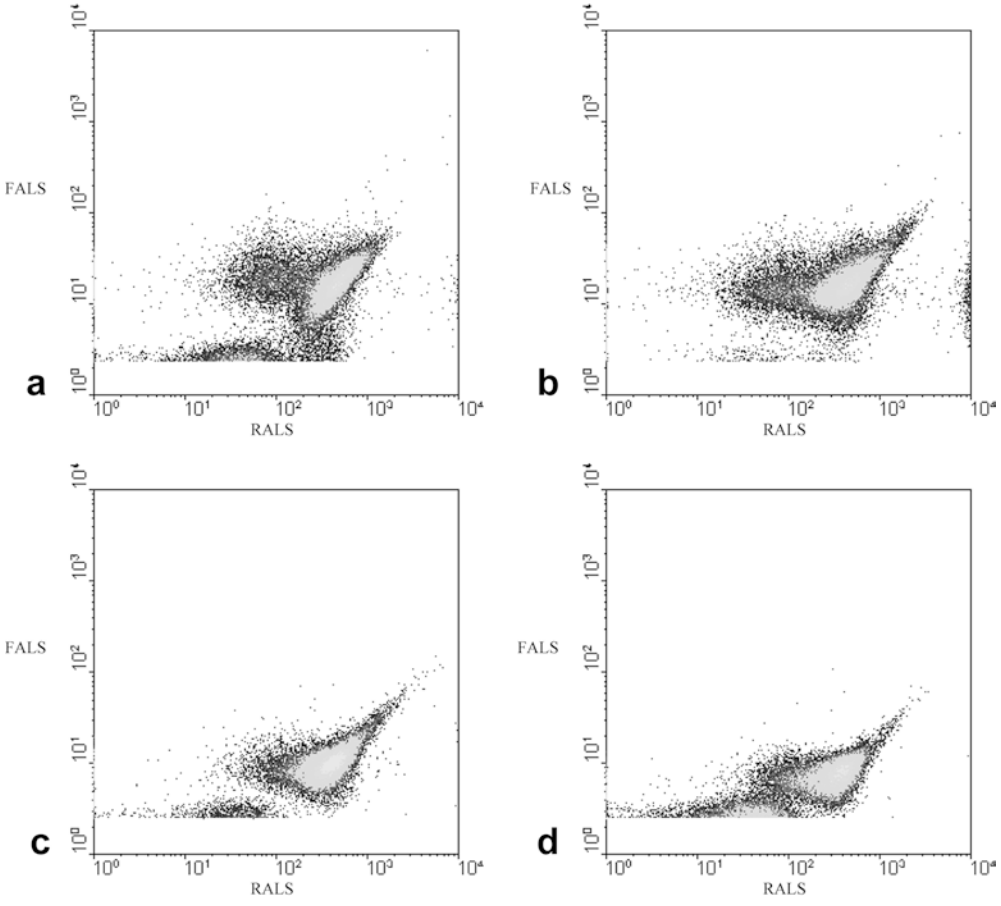

Fig. 6 a–d Changes in the intrinsic light scattering for *E. coli* MSD3735 during the course of a batch fermentation where synthesis of AP50 was not induced. Time during fementation: **a** 2 h, **b** 4 h, **c** 6 h, **d** 9 h. All illustrate the bimodal clustering characteristic for rod-shaped cells

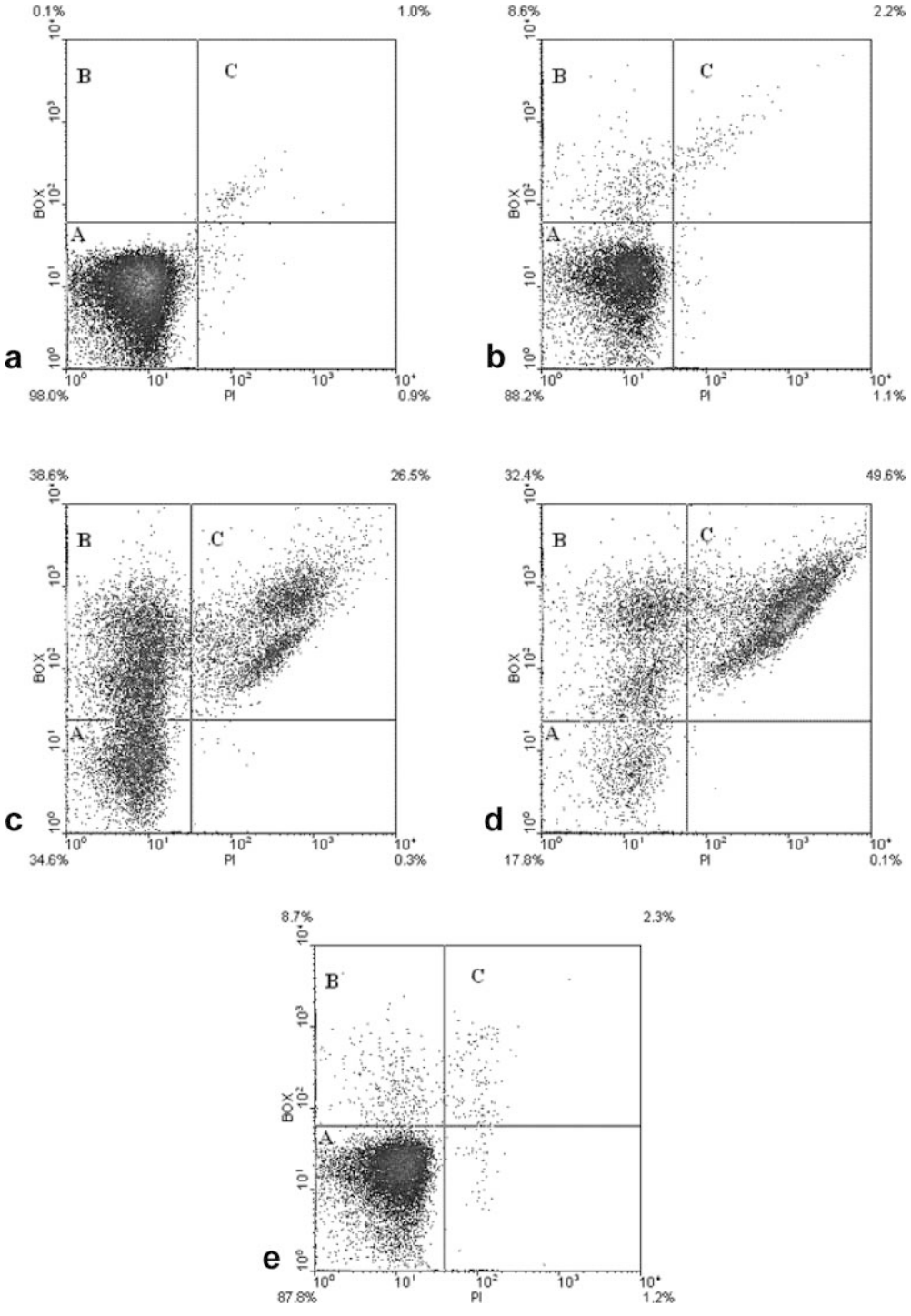

Fig. 7 Cell samples taken: **a** immediately before induction, **b** ca. 1 h after induction, **c** at 3 h, **d** at 15 h and **e** at 20 h during the course of a batch fermentation where synthesis of AP50 was induced at $OD_{550} = 1$. Cells were stained with PIX and up to three main sub-populations of cells can be distinguished, corresponding to: healthy polarised cells (*A*) with no staining, cells with no membrane potential (*B*) and stained with BOX and cells with a depolarised permeabilised cytoplasmic membrane (*C*) and stained with both PI and BOX

and, being a measure of cell granularity, it is sensitive to internal structure. Since the mis-folding of AP50 causes a large phase-bright, refractive inclusion body to accumulate at one end of a distended cell (Fig. 3), an increase in both RALS and FALS should be measurable when compared with a non-producing cell. It has been shown that untransformed *E. coli* cells generate a unimodal distribution with respect to FALS and a bimodal distribution with respect to RALS. This is characteristic for rod-shaped cells because of their rotational asymmetry [10]. In this work, it was shown that, during a recombinant *E. coli* MSD3735 batch fermentation, almost immediately (ca. 1 h) after induction with 0.5 mM IPTG at $OD_{550} \leq 1$ there is a progressive increase in both RALS and FALS signals, which is accompanied by the accumulation of insoluble mis-folded AP50 within the cell (Figs. 4, 5, not all data shown). Further, after 15 h there is the beginning of a return to the bimodal distri-

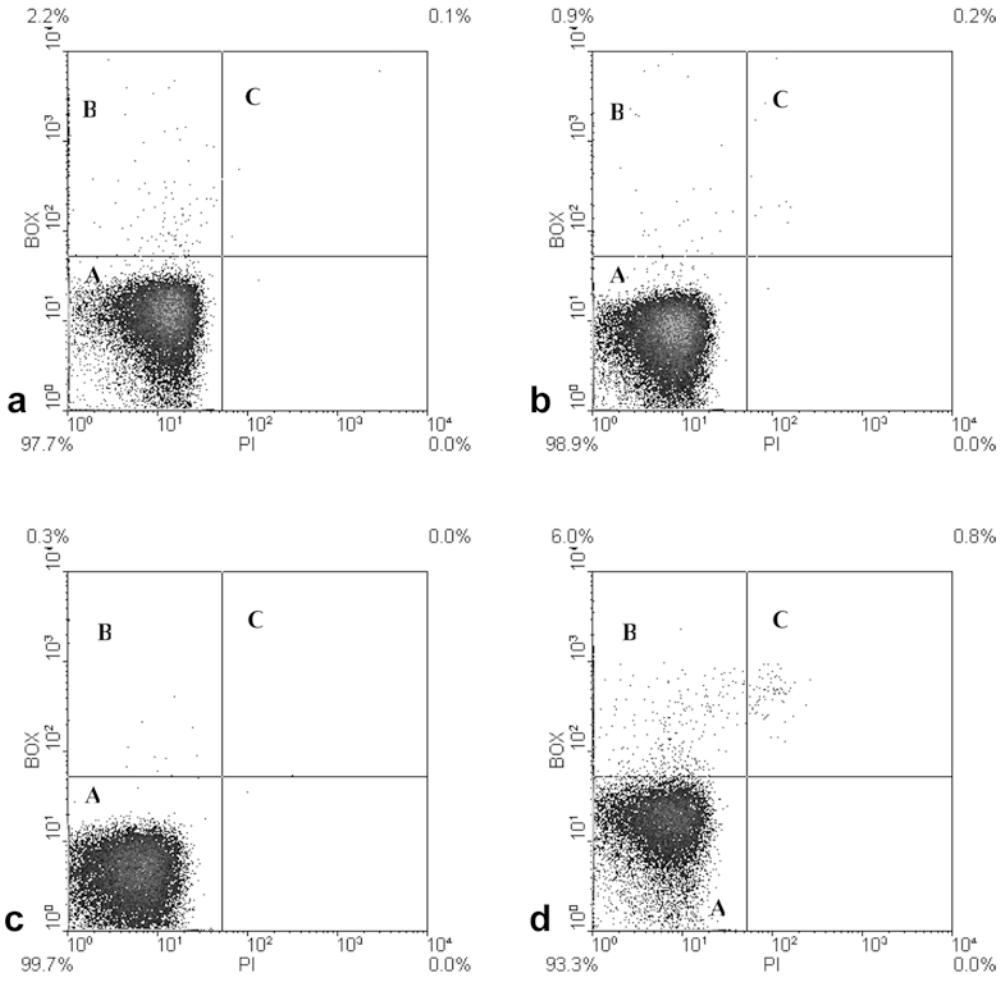

Fig. 8 Cell samples taken at: **a** 2 h, **b** 4 h, **c** 6 h and **d** 9 h during the course of a batch fermentation where synthesis of AP50 was not induced. Stained with PIX, up to three main sub-populations of cells can be distinguished, corresponding to healthy polarised cells (*A*) with no staining, cells with no membrane potential (*B*) and stained with BOX and cells with a depolarised permeabilised cytoplasmic membrane (*C*) and stained with both PI and BOX

bution characteristic of wild-type cells (complete at 20 h); and this is accompanied by the main phase of cell division and the inability of the cells to synthesise either soluble or insoluble AP50. This was confirmed when cells isolated from the fermentation at 20 h and plated onto nutrient agar supplemented with tetracycline formed colonies, indicating that there must have been some form of structural instability within the foreign gene sequence rather than plasmid loss for AP50 not to be expressed. Indeed, a new band appears on the analysis gels, indicating that an unidentified protein is being expressed instead of the target AP50 (Fig. 5). Light scatter data similar to those obtained for these fermentations were obtained for all other fermentations induced with IPTG in the range $OD_{550} = 5$–15 using the recombinant strain of *E. coli* MSD3735, although no structural instabilities within the foreign gene sequence were observed and there was no return to the bimodal distribution characteristic of wild-type cells. In contrast, throughout the course of the experiments where IPTG was added to a batch fermentation of the untransformed host at $OD_{550} = 0.1$ (data not shown) and not added at all to a batch fermentation of the recombinant strain, relatively little change in either RALS or FALS was measurable (Fig. 6).

Fluorescent staining

Analysis of the fluorescent staining data as measured by flow cytometry is very interesting. In all cases, immediately after the addition of the IPTG there begins a progressive change in the cell physiological state that continues throughout the course of each fermentation; and the extent of this is dependent on the OD_{550} at which the IPTG was added, as revealed by PIX staining (BOX and PI together). As described previously [10–13], Fig. 7 shows three distinct areas: area A (with no staining) represents healthy cells, area B (stained with BOX) shows cells with a reduced cytoplasmic membrane potential (stressed cells) and area C (PIX-stained) shows cells with a depolarised permeabilised cytoplasmic membrane (dead cells). For the cases where IPTG was added at $OD_{550} \leq 1$, the number of cells identified as either being stressed or dead increased to a maximum of ca. 50% at 15 h (Fig. 7, not all data shown) and then progressively decreased as the cells began to grow and divide, until reaching a minimum of $\leq 10\%$ (i.e. ca. 90% healthy cells) at the termination of the fermentation. During this period, those healthy cells producing the unknown protein may have a competitive advantage over and

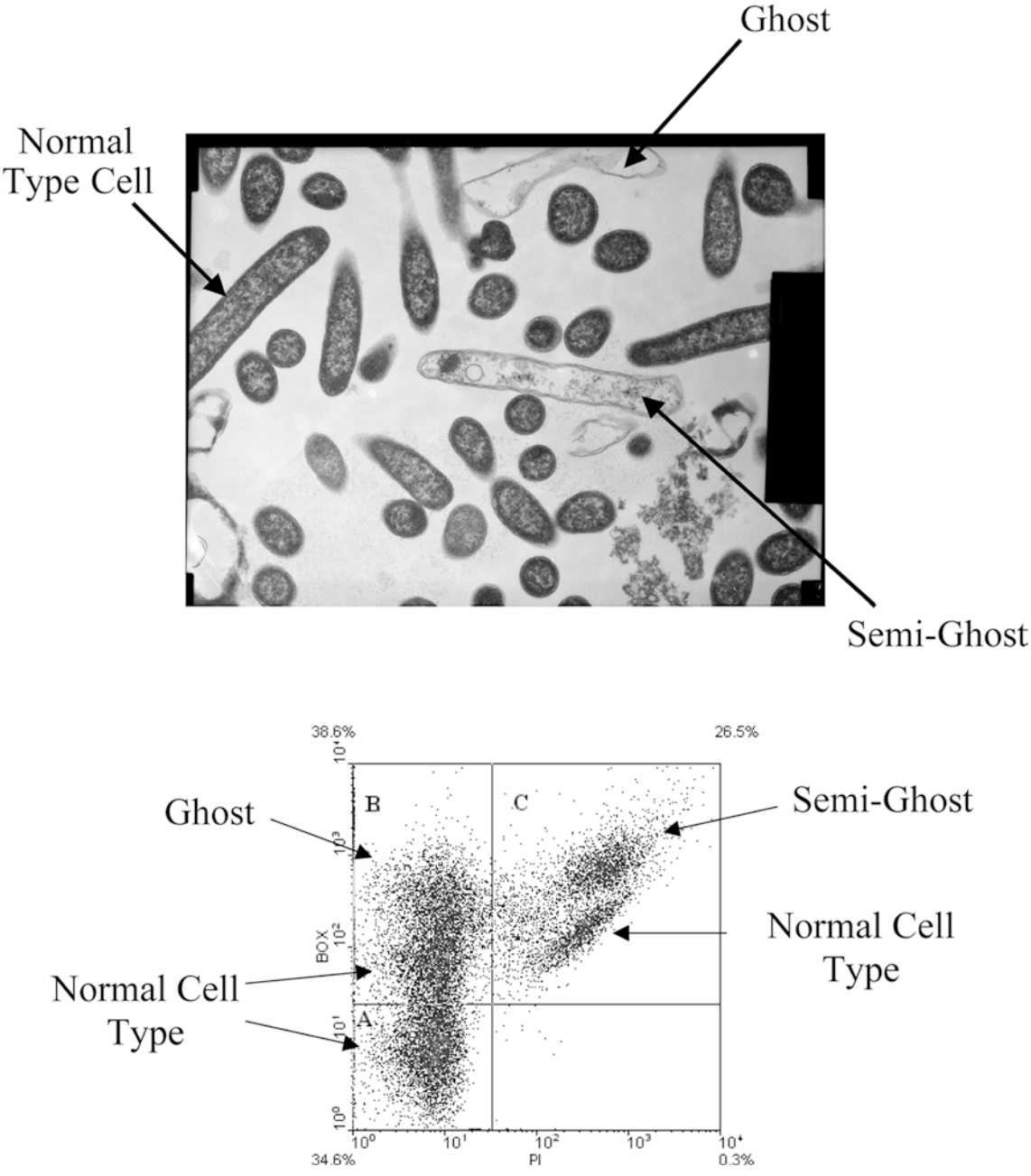

Fig. 9 A representative TEM (×25,000) of cell samples taken 15 h after the synthesis of AP50 was induced at $OD_{550} = 1$. This illustrates the three types of cell ("normal", semi-ghost, ghost), the presence of which may give rise to the measurable differential fluorescence of BOX-positive cells observed in Fig. 7a,b. The former is reproduced here for clarity

probably outgrow those expressing AP50. It is unclear whether such cells are present at the start of the fermentation or are produced in response to the induction process at low OD_{550}(0.1, 0.5, 1.0) and when the growth rates are slow. However, the latter case would seem more likely, since such cells are not found when the system is induced at higher OD_{550}(5, 15). For the cases of fermentations where IPTG was added at $OD_{550} = 5$ or 15 (data not shown), the number of cells identified as either being stressed or dead increased to a maximum of 40% at the termination of the fermentation. In contrast, throughout the course of the experiments where IPTG was added to a batch fermentation of the untransformed host at $OD_{550} = 0.1$ (data not shown) and not added at all to a batch fermentation of the recombinant strain, there was virtually no change in physiological state as measured by PIX staining, with stressed or dead cells only just starting to appear at the termination of the fermentation when glycerol was exhausted (Fig. 8). The distinctive clustering of BOX- and PIX-positive cells is very interesting and deserves further discussion. In all cases, positively stained cell sub-populations can be divided into two further sub-populations, based on

their relative BOX fluorescent-staining intensities. On examination of the culture broth using TEM (Fig. 9), it became clear that "cell type" structures existed in the broth that had little (semi-ghost) and no (ghost) cytoplasmic material inside the cell envelope. It is thought that, where the contents of the cell leak out, more lipophilic binding sites may become available and BOX fluorescence enhanced [17]. Where the contents of the cell entirely leak out (i.e. no nucleic acid remaining), cells are only enhanced BOX-positive and PI-negative, whilst cells in which nucleic acid still remains are enhanced BOX- and normal PI-positive. If this is the case, our estimates of the number of dead cells in each corresponding fermentation process are too low and the number of ghosts needs to be included to give the true value.

Conclusions

This work confirms the findings of others [9, 15, 22] that it is possible to follow inclusion body formation following induction by intrinsic light scatter alone throughout the course of batch fermentations with recombinant *E. coli* MSD3735 producing AP50. Importantly, it goes further in discussing the effect that the expression of a heterologous recombinant protein as inclusion bodies has on the individual cell physiological state. From the data presented here, it is obvious that the expression of AP50 as an insoluble inclusion body, measured either by changes in intrinsic light scatter or by conventional gel electrophoresis, correlates very well with any detrimental change in cell physiological state as measured by PIX staining and, further, that such expression exerts a profound physiological stress on the host cell. However, it is possible that this stress is due simply to the rather large physical presence of the inclusion body and is not due to the metabolic load of having to synthesise the foreign protein. Those cells producing the unidentified protein in fermentations that were induced at $OD_{550} \leq 1$ (after 15 h) remained healthy throughout.

The ability to make such measurements rapidly is important for a fermentation process like this, where it is possible to either increase or decrease inclusion body formation by manipulating the fermentation conditions. Typically, inclusion body formation can be avoided if the fermentation is carried out at lower temperatures (20°C) or if the concentration of the inducer is reduced. Clearly, if the fermentation is carried out at a sub-optimal temperature with respect to growth, the process will take longer. Therefore, the rapid (within minutes), reliable screening of 50,000 cells for the presence of inclusion bodies by flow cytometry allows the fermentation protocol to be optimised (in real time) for growth before induction and then manipulated after induction when the presence of low levels of inclusion body are detected. In this way, the accumulation of mis-folded inactive protein can be avoided, but at optimal growth rates. This is not possible with the slower conventional SDS-PAGE or traditional biochemical assays of protein accumulation, where results are often available too late for the engineer to make any meaningful changes to the process.

Acknowledgements This work was funded by the British Biotechnology and Biological Research Council and AstraZeneca, Alderly Park, Macclesfield, United Kingdom.

References

1. Baneyx F (1999) Recombinant protein expression in *Escherichia coli*. Curr Opin Biotechnol 10:411–421
2. Bentley WE, Mirjalili N, Andersen DC, Davis RH, Kompala D (1990) Plasmid encoded protein: the principle factor in the 'metabolic burden' associated with recombinant bacteria. Biotechnol Bioeng 35:668–661
3. Borth N, Mitterbauer R, Mattanovich D, Kramer W, Bayer K, Katinger H (1998) Flow cytometric analysis of bacterial physiology during induction of foreign protein synthesis in recombinant *Escherichia coli* cells. Cytometry 31:125–129
4. Brinkman U, Mattes RE, Buckel P (1989) High-level expression of recombinant genes in *Escherichia coli* is dependent on the availability of the *dnaY* gene product. Gene 85:109–114
5. Bylund F, Collet E, Enfors SO, Larsson G (1998) Substrate gradient formation in the large-scale bioreactor lowers cell yield and increases by-product formation. Bioprocess Eng 18:171–180
6. Einsele A (1978) Scaling-up of bioreactors. Proc Biochem 13:13–14
7. Enfors SO, Jahic M, Rozkov A, Xu B, Hecker M, Jurgen B, Kruger E, Schweder T, Hamer G, O'Beirne D, Noisommit-Rizzi N, Reuss M, Boon L, Hewitt C, McFarlane C, Nienow A, Fuchs L, Kovacs T, Revstedt J, Tragardh C, Friberg PC, Hjertager B, Blomsten G, Skogman H, Hjort S, Hoeks F, Lin HY, Neubauer P, Lans R van der, Luyben K, Vrabel P, Manelius A (2001) Physiological responses to mixing in large-scale bioreactors. J Biotechnol 85:175–185
8. Follows ER, McPheat JC, Minshull C, Moore NC, Pauptit RA, Rowsell S, Stacey CL, Stanway JJ, Taylor IWF, Abbott WM (2001) Study of the interaction of the medium chain $\mu 2$ subunit of the clathrin associated adaptor protein complex 2 with cytotoxic T-lyphocyte antigen 4 and CD28. Biochem J 359:427–434
9. Fouchet P, Manin C, Richard H, Frelat G, Barbotin JN (1994) Flow cytometry studies of recombinant *Escherichia coli* in batch and continuous cultures: DNA and RNA contents; light-scatter parameters. Appl Microbiol Biotechnol 41:584–590
10. Hewitt CJ, Nebe-von-Caron G, Nienow AW, McFarlane CM (1999a) The use of multi-staining flow cytometry to characterise the physiological state of *Escherichia coli* W3110 in high cell density fed-batch cultures. Biotechnol Bioeng 63:705–711
11. Hewitt CJ, Nebe-von-Caron G, Nienow AW, McFarlane CM (1999b) The use of multi-parameter flow cytometry to compare the physiological response of *Escherichia coli* W3110 to glucose limitation during batch, fed-batch and continuous culture cultivations. J Biotechnol 75:251–264
12. Hewitt CJ, Nebe-von-Caron G, Axelsson B, McFarlane CM, Nienow AW (2000) Studies related to the scale-up of high cell density *E. coli* fed-batch fermentations using multi-parameter flow cytometry: effect of a changing micro-environment with respect to glucose and dissolved oxygen concentration. Biotechnol Bioeng 70:381–390
13. Hewitt CJ, Nebe-von-Caron G (2001) An industrial application of multi-parameter flow cytometry: assessment of cell physiological state and its application to the study of microbial fermentations. Cytometry 44:179–187

14. Laemmli UK (1970) Cleavage of structural proteins during assembly of the head of bacteriophage T4. Nature 227:680–685
15. Lavergne-Mazeau F, Maftah A, Centatiempo Y, Julien R (1996) Linear correlation between bacterial overexpression of recombinant peptides and light scatter. Appl Environ Microbiol 62:3042–3046
16. Nebe-von-Caron G, Badley RA (1995) Viability assessment of bacteria in mixed populations using flow-cytometry. J Microsc (Oxford) 179:55–66
17. Nebe-von-Caron G, Stephens PJ, Hewitt CJ, Powell JR, Badley RA (2000) Analysis of bacterial function by multi-colour and single cell sorting. J Microsc Methods 42:97–114
18. Nienow AW (1998) Hydrodynamics of stirred bioreactors. Appl Mech Rev 51:3–32
19. Onyeaka H, Nienow AW, Hewitt CJ (2003) Further studies related to the scale-up of high cell density *Escherichia coli* fed-batch fermentations: the additional effect of a changing micro-environment when using aqueous ammonia to control pH. Biotechnol Bioeng 84:474–484
20. Oosterhuis NMG, Kossen NWF (1984) Dissolved oxygen concentration profiles in a production scale bioreactor. Biotechnol Bioeng 26:546–550
21. Schweder T, Krüger E, Xu B, Jürgen B, Mostertz J, Blomsten G, Enfors SO, Hecker M (1999) Monitoring of genes that respond to process related stress in large-scale bioprocesses. Biotechnol Bioeng 65:151–159
22. Wittrup KD, Mann MB, Fenton DM, Tsai LB, Bailey JE (1988) Single-cell light scatter as a probe of refractile body formation in recombinant *Escherichia coli*. Bio/Technology 6:423–426
23. Xu B, Jahic M, Blomsten G, Enfors SO (1999) Glucose overflow metabolism and mixed-acid fermentation in aerobic large-scale fed-batch processes with *Escherichia coli*. Appl Microbiol Biotechnol 51:564–571